

The effect of nonlinear mode coupling on the stability of toroidal Alfvén eigenmodes

C. N. Lashmore-Davies, A. Thyagaraja, and R. A. Cairns

Citation: *Phys. Plasmas* **4**, 3243 (1997); doi: 10.1063/1.872466

View online: <http://dx.doi.org/10.1063/1.872466>

View Table of Contents: <http://pop.aip.org/resource/1/PHPAEN/v4/i9>

Published by the [American Institute of Physics](#).

Related Articles

Electric and magnetic contributions to spatial diffusion in collisionless plasmas

Phys. Plasmas **19**, 102309 (2012)

Phase slips and dissipation of Alfvénic intermediate shocks and solitons

Phys. Plasmas **19**, 092116 (2012)

Alfvén's critical ionization velocity observed in high power impulse magnetron sputtering discharges

Phys. Plasmas **19**, 093505 (2012)

Cherenkov radiation of shear Alfvén waves in plasmas with two ion species

Phys. Plasmas **19**, 092109 (2012)

Nonlinear dissipation of circularly polarized Alfvén waves due to the beam-induced obliquely propagating waves

Phys. Plasmas **19**, 082317 (2012)

Additional information on Phys. Plasmas

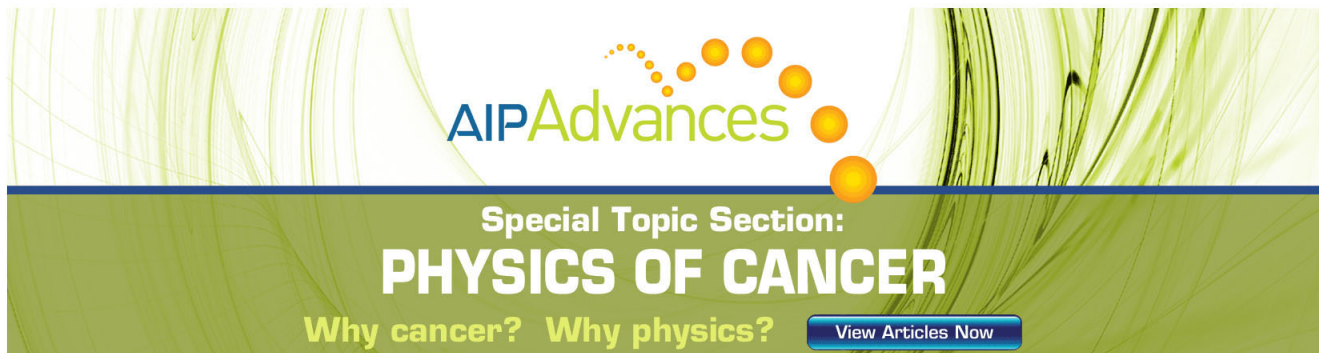
Journal Homepage: <http://pop.aip.org/>

Journal Information: http://pop.aip.org/about/about_the_journal

Top downloads: http://pop.aip.org/features/most_downloaded

Information for Authors: <http://pop.aip.org/authors>

ADVERTISEMENT



AIP Advances

Special Topic Section:
PHYSICS OF CANCER

Why cancer? Why physics? [View Articles Now](#)

The effect of nonlinear mode coupling on the stability of toroidal Alfvén eigenmodes

C. N. Lashmore-Davies and A. Thyagaraja

UKAEA Fusion, Culham, Abingdon, Oxon, OX14 3DB, United Kingdom (UKAEA/Euratom Fusion Association)

R. A. Cairns

School of Mathematical and Computational Sciences, University of St. Andrews, St. Andrews, Fife, KY16 9SS, United Kingdom

(Received 14 February 1997; accepted 11 June 1997)

A cylindrical model of a tokamak is used to describe the nonlinear coupling between Alfvén waves and sound waves. The model is applied to the case of a toroidal Alfvén eigenmode (TAE) driven unstable by fusion alpha particles to explore its relevance to the nonlinear saturation of such modes, which can produce a loss of alpha particles in a burning plasma. The mechanism is the modulational instability of a finite-amplitude wave, in this case a TAE mode, in which a density fluctuation and Alfvén sidebands are spontaneously excited when the finite-amplitude wave exceeds a threshold amplitude. In general, such a nonlinear calculation in a bounded inhomogeneous plasma would require a numerical solution. However, in the present case, an approximate analytic solution is derived by making use of the fact that the sound wave is logarithmically singular on a particular magnetic surface. The calculation is therefore carried out on the magnetic surface on which the TAE instability is centered and a nonlinear dispersion relation is derived. The threshold for the modulational instability yields a value for the ratio of the perturbed radial component of the magnetic field to the equilibrium magnetic field, which is comparable to the saturated amplitude of a TAE instability obtained by other workers. In addition, the nonlinear dispersion relation also includes a resonant case for which the threshold can be significantly lower. The present, heuristic calculation suggests that the modulational instability may indeed be relevant to the evolution and eventual saturation of a TAE instability.

[S1070-664X(97)03109-1]

I. INTRODUCTION

Shear Alfvén waves are modes of a magnetized plasma. For the ideal magnetohydrodynamic (MHD) model in cylindrical geometry shear Alfvén waves form a continuous spectrum. When toroidal effects are included two neighboring poloidal harmonics are coupled, producing a gap in the continuous spectrum and resulting in a mode in this frequency gap.¹ These gap modes are referred to as toroidal Alfvén eigenmodes (TAE). Because a TAE mode occurs in a gap in the continuous spectrum, it is less susceptible to continuum damping and is therefore a likely candidate for instability. In particular, Fu and Van Dam² have shown that TAE modes can be driven unstable by resonant interaction with fusion alpha particles that are concentrated in the center of a discharge, the region where they are predominantly born. Such TAE instabilities driven by fusion alpha particles have recently been identified³ in the Tokamak Fusion Test Reactor (TFTR),⁴ although no associated loss of alpha particles was observed. It is believed that alpha-particle-driven TAE instabilities are likely to occur in the International Thermonuclear Experimental Reactor⁵ (ITER), which may be a threat to alpha-particle confinement in ITER. A question that then arises is what are the possible saturation mechanisms of these instabilities and what is the resulting saturation amplitude. This is an important question, since if the saturated amplitude of the fluctuating magnetic field is too high, the instability would produce rapid loss of the energetic alpha

particles, resulting in a significant reduction in the heating to which these particles would otherwise contribute.

There are a number of possible saturation mechanisms. One such mechanism is the trapping of the alpha particles in the finite wave amplitude. This process has been analyzed by Berk and Breizman.⁶ Another class of saturation mechanisms involves the excitation of other waves by the large-amplitude field that results from the instability. The energy that drives the instability is therefore transferred to other modes of oscillation, resulting in saturation of the finite-amplitude mode.

Calculations of this type have been carried out by Vlad *et al.*,⁷ Spong *et al.*,⁸ and Hahm and Chen.⁹ In the latter calculation two different TAE modes, centered on neighboring magnetic surfaces, beat to produce a low-frequency density perturbation. The unstable TAE modes are therefore saturated by the excitation of a spectrum of density perturbations.

The present calculation is related to that of Ref. 9, in so far as the energy from the TAE instability is coupled to a low-frequency density perturbation. However, the mechanism to be described in this paper possesses a number of significant differences. The first is that it only requires a single TAE mode. It does not even require explicit recognition of the existence of two coupled poloidal harmonics other than to specify the frequency of the TAE mode. In Ref. 9, the two independent TAE modes on neighboring magnetic surfaces are required to have significant spatial overlap. This is not required in the present calculation, which refers only to

the magnetic surface on which the TAE mode is centered. Whereas the density perturbation discussed in Ref. 9 is a driven mode requiring both TAE modes to reach a rather large amplitude, $\delta B_r/B_0 \leq 10^{-3}$, the density perturbation considered here arises spontaneously when the TAE mode exceeds a critical amplitude. Such nonlinear finite-amplitude instabilities of Alfvén waves have been analyzed earlier for simple uniform plasmas.^{10,11}

In general, the calculation of such nonlinear couplings in a nonuniform plasma is extremely involved and would require a numerical solution of the governing equations. However, there is one special feature of low-frequency sound waves in ideal magnetohydrodynamics (MHD), which enables an approximate analytic calculation to be carried out. Such a calculation provides insight into the relevance of such finite amplitude instabilities as saturation mechanisms. The feature utilized is that sound waves form a continuum of modes, each of which propagates along the equilibrium magnetic field with a frequency and parallel wavelength corresponding to the sound speed associated with a particular magnetic surface. The mechanism to be analyzed here can be described as follows.

Consider the magnetic surface where two poloidal harmonics (m_a, n_a) and $(m_a + 1, n_a)$ are coupled toroidally to produce an Alfvén gap mode. The TAE mode is therefore centered on the $q = (m_a + \frac{1}{2})/n_a$ surface and is assumed to be driven unstable, for example, by energetic alpha particles. A low-frequency sound fluctuation with frequency ω and poloidal and toroidal mode numbers (m_h, n_h) is assumed to occur on the same magnetic surface. Initially, the low-frequency sound perturbation is at noise level. The finite-amplitude Alfvén wave beats with the sound perturbation to produce sidebands with frequency $\omega_a \pm \omega$ and wave numbers $\mathbf{k}_a \pm \mathbf{k}_h$. In general, these sidebands will be driven, or forced, modes but they can also beat with the finite-amplitude TAE mode to reinforce the low-frequency sound perturbation, thus closing the feedback loop. Following this procedure an equation for the low-frequency sound wave can be obtained that contains an additional term proportional to the intensity of the TAE wave. This equation can be linearized by assuming the amplitude of the TAE mode is much larger than the amplitudes of the other perturbations. With this assumption the equation can be solved for the threshold of the modulational instability of the TAE mode.

The significance of this mechanism for the saturation of a TAE instability is as follows. A TAE instability will grow until its amplitude reaches the threshold for the modulational instability. At this amplitude, the TAE instability will cause a low-frequency density fluctuation and Alfvén sidebands to begin to grow. The energy driving the original TAE instability will now be transferred to these other fluctuations and there will be no further growth of the TAE wave amplitude that will remain close to the modulational threshold.

In carrying out this procedure a number of approximations must be made. The most important of these is the retention of only those coupling terms that yield the highest (namely second) radial derivatives of the amplitude of the low-frequency perturbation because it is singular. The final result comes from the consistency condition that the modi-

fied low-frequency fluctuation should be singular at the position of the maximum of the TAE wave, i.e. that the coefficient of the second-order derivative should equal zero on the magnetic surface on which the TAE mode is centered. The essential assumption is that the TAE wave and all the coupled modes should have radial eigenfunctions that are highly localized on the original magnetic surface. Our final result shows that the effect is most significant for high values of m_a for which the assumption of radial localization is well satisfied.

The plan of the paper is as follows. In Sec. II it is argued that the cylindrical, screw pinch model is an adequate approximation of the tokamak to represent the nonlinear coupling. A toroidal model is only required to establish the finite-amplitude TAE mode, but is not necessary for the nonlinear coupling. The equations of ideal MHD are written in a form with the linear terms on the left-hand side and the nonlinear coupling terms on the right-hand side. These equations are then used to obtain a generalized Hain–Lüst¹² equation that is modified from the linear version by the inclusion of the nonlinear coupling terms. In Sec. III the nonlinear Hain–Lüst equation is used to obtain the equations for the sidebands and the equation for the low-frequency density perturbation. In Sec. IV we describe the approximate integration of the sideband equations and the derivation of the final form of the low-frequency equation, which then yields the dispersion relation for the modulational instability of the TAE mode. A summary and conclusions are given in Sec. V.

II. THE NONLINEAR MODIFICATION OF THE HAIN–LÜST EQUATION

The aim of this calculation is to obtain an estimate for the critical amplitude of a toroidal Alfvén eigenmode to become modulationally unstable. If this amplitude is low enough, then this mechanism could be important in determining the saturated amplitude of a TAE mode driven unstable by fusion alpha particles. In order to describe this process we must use the compressible equations of ideal MHD so that the sound waves are included in the model. However, the nonlinear coupling mechanism considered here does not depend on toroidal effects. It is therefore sufficient to analyze a cylindrical model of a tokamak plasma. For this purpose it is convenient to consider the screw pinch where the linearized eigenmode equation was first obtained by Hain and Lüst.¹² In deriving a nonlinear version of this equation, the method and notation given by Freidberg¹³ has been closely followed. The equations of ideal MHD can be written as

$$\rho \frac{\partial \mathbf{v}}{\partial t} + \rho(\mathbf{v} \cdot \nabla) \mathbf{v} = -\nabla p + \frac{1}{\mu_0} (\nabla \times \mathbf{B}) \times \mathbf{B}, \quad (1)$$

$$\frac{\partial \rho}{\partial t} + \nabla \cdot (\rho \mathbf{v}) = 0, \quad (2)$$

$$\left(\frac{\partial}{\partial t} + \mathbf{v} \cdot \nabla \right) \left(\frac{p}{\rho^\gamma} \right) = 0, \quad (3)$$

$$\frac{\partial \mathbf{B}}{\partial t} = \nabla \times (\mathbf{v} \times \mathbf{B}), \quad (4)$$

where ks units are used and all symbols have their usual meaning. These are the fully nonlinear equations. The variables \mathbf{v} , \mathbf{B} , ρ , and p are now written as a sum of an equilibrium part and a perturbation, i.e.

$$\mathbf{B} = \mathbf{B}_0 + \mathbf{B}_1. \quad (5)$$

Note that there is no equilibrium flow, i.e. $\mathbf{v}_0 = 0$. The governing equations are now written with the linear terms on the left-hand side and the nonlinear terms on the right-hand side, giving

$$\begin{aligned} \rho_0 \frac{\partial v_1}{\partial t} + \nabla p_1 - \frac{1}{\mu_0} (\nabla \times \mathbf{B}_0) \times \mathbf{B}_1 - \frac{1}{\mu_0} (\nabla \times \mathbf{B}_1) \times \mathbf{B}_0 \\ = -\rho_1 \frac{\partial \mathbf{v}_1}{\partial t} - \rho_0 (\mathbf{v}_1 \cdot \nabla) \mathbf{v}_1 + \frac{1}{\mu_0} (\nabla \times \mathbf{B}_1) \times \mathbf{B}_1, \end{aligned} \quad (6)$$

$$\frac{\partial \rho_1}{\partial t} + \nabla \cdot (\rho_0 \mathbf{v}_1) = -\nabla \cdot (\rho_1 \mathbf{v}_1), \quad (7)$$

$$\frac{\partial \mathbf{B}_1}{\partial t} - \nabla \times (\mathbf{v}_1 \times \mathbf{B}_0) = \nabla \times (\mathbf{v}_1 \times \mathbf{B}_1), \quad (8)$$

$$\begin{aligned} \frac{\partial}{\partial t} \left(\frac{p_1}{\rho_0^\gamma} - \frac{\gamma p_0}{\rho_0^{\gamma+1}} \rho_1 \right) + (\mathbf{v}_1 \cdot \nabla) \frac{p_0}{\rho_0^\gamma} \\ = -(\mathbf{v}_1 \cdot \nabla) \frac{p_1}{\rho_0^\gamma} + (\mathbf{v}_1 \cdot \nabla) \frac{\gamma p_0}{\rho_0^{\gamma+1}} \rho_1 + \frac{\gamma}{\rho_0^{\gamma+1}} \frac{\partial}{\partial t} (p_1 \rho_1) \\ - \frac{\gamma(\gamma+1)}{2} \frac{p_0}{\rho_0^{\gamma+2}} \frac{\partial}{\partial t} \rho_1^2, \end{aligned} \quad (9)$$

where we have retained only quadratic nonlinearities. Following the procedure outlined in Ref. 13, we introduce the plasma displacement vector ξ , where

$$\mathbf{v}_1 = \frac{\partial \xi}{\partial t}. \quad (10)$$

The displacement ξ is decomposed into the vector components

$$\xi = \xi_r \hat{e}_r + \eta \hat{e}_\eta + \xi_\parallel \hat{b}. \quad (11)$$

Similarly,

$$\mathbf{B}_1 = B_{1r} \hat{e}_r + B_\eta \hat{e}_\eta + B_\parallel \hat{b}, \quad (12)$$

where

$$\hat{b} = (B_{0\theta} \hat{e}_\theta + B_{0z} \hat{e}_z) / B_0, \quad (13)$$

$$\hat{e}_\eta = (B_{0z} \hat{e}_\theta - B_{0\theta} \hat{e}_z) / B_0, \quad (14)$$

$$B_0 = (B_{0\theta}^2 + B_{0z}^2)^{1/2},$$

and \hat{e}_r is the unit vector in the radial direction.

Using Eqs. (10)–(14), we can obtain the variables B_η and B_\parallel from Eq. (8), giving

$$\begin{aligned} B_\eta = iF_\eta + \xi_r \left[\frac{B_{0\theta} B'_{0z}}{B_0} - \frac{r B_{0z}}{B_0} \left(\frac{B_{0\theta}}{r} \right)' \right] \\ - i \frac{B_{0z}}{\omega B_0} \frac{\partial}{\partial r} \left(B_{1\theta} \frac{\partial \xi_r}{\partial t} - B_{1r} \frac{\partial \xi_\theta}{\partial t} \right) \\ - i \frac{B_{0\theta}}{\omega B_0} \frac{1}{r} \frac{\partial}{\partial r} \left[r \left(B_{1r} \frac{\partial \xi_z}{\partial t} - B_{1z} \frac{\partial \xi_r}{\partial t} \right) \right], \end{aligned} \quad (15)$$

$$\begin{aligned} B_\parallel = -iG_\eta - \frac{B_0}{r} (r\xi_r)' + \frac{\xi_r}{B_0} \left(\mu_0 p_0' + \frac{2B_{0\theta}^2}{r} \right) \\ - i \frac{B_{0\theta}}{\omega B_0} \frac{\partial}{\partial r} \left(B_{1\theta} \frac{\partial \xi_r}{\partial t} - B_{1r} \frac{\partial \xi_\theta}{\partial t} \right) \\ + i \frac{B_{0z}}{\omega B_0} \frac{1}{r} \frac{\partial}{\partial r} \left[r \left(B_{1r} \frac{\partial \xi_z}{\partial t} - B_{1z} \frac{\partial \xi_r}{\partial t} \right) \right]. \end{aligned} \quad (16)$$

The prime in Eqs. (15) and (16) denotes a radial derivative. The equations for B_η and B_\parallel consist of the linear terms given in Ref. 13 with additional nonlinear terms. Only the nonlinear terms with radial derivatives have been included in Eqs. (15) and (16) for reasons to be discussed below. The equation for B_{1r} is unchanged since the nonlinear terms in the radial component of Eq. (8) do not involve any radial derivatives. Thus

$$B_{1r} = iF\xi_r. \quad (17)$$

The quantities F and G are given by

$$F = kB_{0z} + \frac{m}{r} B_{0\theta}, \quad (18)$$

$$G = \frac{m}{r} B_{0z} - kB_{0\theta}, \quad (19)$$

where all perturbed quantities vary as $Q_1 = Q_1(r) \exp[i(m\theta + kz - \omega t)]$.

The next step is to use the equation of motion to obtain equations for η and ξ_\parallel in terms of ξ_r and $(r\xi_r)'$ and the corresponding nonlinear coupling terms. The equations for η and ξ_\parallel are as follows:

$$\begin{aligned} -\omega^2 \rho_0 \eta = -\frac{iG}{B_0} \left(p_1 + \frac{B_0 B_\parallel}{\mu_0} \right) + \frac{iF}{\mu_0} B_\eta \\ + \frac{B_{0z}}{B_0} \left(\frac{B_{0\theta}}{\mu_0 r} + \frac{B'_{0\theta}}{\mu_0} \right) B_{1r} - \frac{B_{0\theta} B'_{0z}}{B_0 \mu_0} B_{1r} \\ - \frac{B_{0z}}{B_0} \rho_1 \frac{\partial^2 \xi_\theta}{\partial t^2} - \frac{B_{0z}}{B_0} \rho_0 \frac{\partial \xi_r}{\partial t} \frac{\partial}{\partial r} \frac{\partial \xi_\theta}{\partial t} \\ + \frac{B_{0z}}{B_0} \frac{B_{1r}}{\mu_0} \frac{1}{r} \frac{\partial}{\partial r} (rB_{1\theta}) + \frac{B_{0\theta}}{B_0} \rho_1 \frac{\partial^2 \xi_z}{\partial t^2} \\ + \frac{B_{0\theta}}{B_0} \rho_0 \frac{\partial \xi_r}{\partial t} \frac{\partial}{\partial r} \frac{\partial \xi_z}{\partial t} - \frac{B_{0\theta} B_{1r}}{B_0 \mu_0} \frac{\partial B_{1z}}{\partial r}, \end{aligned} \quad (20)$$

$$\begin{aligned}
-\omega^2 \rho_0 \xi_{\parallel} = & -\frac{iF}{B_0} p_1 + \frac{B_{0\theta}}{B_0} \left(\frac{B_{0\theta}}{\mu_0 r} + \frac{B'_{0\theta}}{\mu_0} \right) B_{1r} \\
& + \frac{B_{0z}}{B_0} \frac{B'_{0z}}{\mu_0} B_{1r} - \frac{B_{0\theta}}{B_0} \rho_1 \frac{\partial^2 \xi_{\theta}}{\partial t^2} \\
& - \frac{B_{0\theta}}{B_0} \rho_0 \frac{\partial \xi_r}{\partial t} \frac{\partial}{\partial r} \frac{\partial \xi_{\theta}}{\partial t} \\
& + \frac{B_{0\theta}}{B_0} \frac{B_{1r}}{\mu_0 r} \frac{\partial}{\partial r} (r B_{1\theta}) - \frac{B_{0z}}{B_0} \rho_1 \frac{\partial^2 \xi_z}{\partial t^2} \\
& - \frac{B_{0z}}{B_0} \rho_0 \frac{\partial \xi_r}{\partial t} \frac{\partial}{\partial r} \frac{\partial \xi_z}{\partial t} + \frac{B_{0z}}{B_0} \frac{B_{1r}}{\mu_0} \frac{\partial B_{1z}}{\partial r}. \quad (21)
\end{aligned}$$

Note that Eqs. (20) and (21) also contain nonlinear coupling terms proportional to $\rho_1(\partial^2 \xi_{\theta}/\partial t^2)$ and $\rho_1(\partial^2 \xi_z/\partial t^2)$. These have been included because such terms were found to be significant in a similar calculation for a uniform plasma.¹¹

Using Eq. (9), we obtain

$$p_1 \approx -p'_0 \xi_r - \gamma p_0 \left(\frac{(r \xi_r)'}{r} + \frac{iG}{B_0} \eta + \frac{iF}{B_0} \xi_{\parallel} \right), \quad (22)$$

where the nonlinear terms have been neglected, since their contribution to the final form of the equations was found to be unimportant. The desired equations for η and ξ_{\parallel} can be put in their final form by substituting Eqs. (15)–(17) and Eq. (22) into Eqs. (20) and (21), giving

$$\begin{aligned}
\left(\frac{\gamma p_0 F G}{B_0^2} \right) \xi_{\parallel} + \left(\frac{k_0^2 B_0^2}{\mu_0} + \frac{\gamma p_0 G^2}{B_0^2} - \omega^2 \rho_0 \right) \eta \\
= \frac{iG(\gamma p_0 + B_0^2/\mu_0)}{r B_0} (r \xi_r)' + \left(\frac{2ik_0 B_0 B_{0\theta}}{\mu_0 r} \right) \xi_r + N, \quad (23)
\end{aligned}$$

$$\left(\frac{\gamma p_0 F^2}{B_0^2} - \omega^2 \rho_0 \right) \xi_{\parallel} + \frac{\gamma p_0 F G}{B_0^2} \eta = \frac{i \gamma p_0 F}{r B_0} (r \xi_r)' + L, \quad (24)$$

where $k_0^2 = k^2 + m^2/r^2$, and L and N are the nonlinear coupling terms coming from Eqs. (15), (16), (20), and (21). The expressions for L and N are given in the Appendix. However, we shall find that the nonlinear coupling is dominated by a small number of terms. To derive the Hain–Lüst equation with its nonlinear modifications, Eqs. (23) and (24) must be solved for η and ξ_{\parallel} , giving

$$\begin{aligned}
\xi_{\parallel} = & \frac{-i \gamma p_0 F}{r \rho_0 B_0 D} \left((\omega^2 - \omega_a^2)(r \xi_r)' + \frac{2k_0 G B_{0\theta}}{\mu_0 \rho_0} \xi_r \right) \\
& + \frac{c_s^2 F G [(\omega_g^2 - \omega^2)N - (k_0^2 c_A^2 + c_s^2 G^2/B_0^2 - \omega^2)L]}{B_0^2 (\omega^2 - \omega_g^2) \rho_0 D}, \quad (25)
\end{aligned}$$

$$\begin{aligned}
\eta = & -\frac{i}{r \rho_0 B_0 D} \left[G \left(\gamma p_0 + \frac{B_0^2}{\mu_0} \right) (\omega^2 - \omega_h^2)(r \xi_r)' \right. \\
& \left. + \frac{2k_0 B_0^2 B_{0\theta}}{\mu_0} (\omega^2 - \omega_g^2) \xi_r \right] \\
& + \frac{[(c_s^2 F G/B_0^2)^2 L - (\omega_g^2 - \omega^2)^2 N]}{\rho_0 (\omega^2 - \omega_g^2) D}, \quad (26)
\end{aligned}$$

where

$$D = (\omega^2 - \omega_f^2)(\omega^2 - \omega_s^2),$$

$$\omega_{f,s}^2 = \frac{1}{2} k_0^2 (c_A^2 + c_s^2) [1 \pm (1 - \alpha^2)^{1/2}],$$

$$\alpha^2 = \frac{4c_s^2 \omega_a^2}{k_0^2 (c_A^2 + c_s^2)^2},$$

$$\omega_a^2 = \frac{F^2}{\mu_0 \rho_0},$$

$$\omega_h^2 = \frac{c_s^2}{(c_s^2 + c_A^2)} \omega_a^2,$$

$$\omega_g^2 = \frac{c_s^2}{c_A^2} \omega_a^2,$$

and

$$c_s^2 = \gamma p_0 / \rho_0, \quad c_A^2 = B_0^2 / \rho_0 \mu_0.$$

The solutions for η and ξ_{\parallel} given in Eqs. (25) and (26) are valid provided $D \neq 0$. We shall return to this point later.

The final form of the nonlinear eigenmode equation is obtained from the radial component of Eq. (6), which is

$$\begin{aligned}
\rho_0 (\omega^2 - \omega_a^2) \xi_r = & \frac{d}{dr} \left(p_1 + \frac{B_0 B_{\parallel}}{\mu_0} \right) + \frac{2B_{0\theta}}{\mu_0 r} \left(\frac{B_{0z}}{B_0} B_{\eta} + \frac{B_{0z} B_{\parallel}}{B_0} \right) \\
& + \frac{B_{1z}}{\mu_0} \frac{\partial B_{1z}}{\partial r} + \frac{B_{1\theta}}{\mu_0} \frac{1}{r} \frac{\partial}{\partial r} (r B_{1\theta}), \quad (27)
\end{aligned}$$

where only those nonlinear terms possessing radial derivatives have been included. Substituting Eqs. (15), (16), (22), and (26) into Eq. (27), we obtain

$$\begin{aligned}
\frac{d}{dr} \left(A \frac{d}{dr} (r \xi_r) \right) - C (r \xi_r) \\
= \frac{B_0}{\mu_0} \frac{d}{dr} \left(M - iG \frac{[(c_s^2 F G/B_0^2)^2 L - (\omega_g^2 - \omega^2)^2 N]}{\rho_0 (\omega^2 - \omega_g^2) D} \right) \\
+ \frac{B_{1\theta}}{\mu_0} \frac{1}{r} \frac{d}{dr} (r B_{1\theta}), \quad (28)
\end{aligned}$$

where M represents the nonlinear terms in Eq. (16). The nonlinear terms in Eq. (28) come from $(d/dr)(B_0 B_{\parallel}/\mu_0)$, except for the last term, which arises from the radial component of the equation of motion. The other nonlinear term in this equation is much smaller and has been neglected. These are the terms that result in coupling terms proportional to the required second-order radial derivatives. The quantities A and C are the same as given by Hain and Lüst,^{12,13} and are

$$A = \left(\frac{\rho_0(c_s^2 + c_A^2)}{r} \right) \frac{(\omega^2 - \omega_a^2)(\omega^2 - \omega_h^2)}{(\omega^2 - \omega_f^2)(\omega^2 - \omega_s^2)}, \quad (29)$$

$$C = -\frac{\rho_0}{r} (\omega^2 - \omega_a^2) + \left(\frac{4k^2 c_A^2 B_{0\theta}^2}{\mu_0 r^3} \right) (\omega^2 - \omega_g^2) + \frac{d}{dr} \left[\frac{B_{0\theta}^2}{\mu_0 r^2} - \left(\frac{2k B_{0\theta} G}{\mu_0 r^2} \right) \frac{(c_s^2 + c_A^2)(\omega^2 - \omega_h^2)}{(\omega^2 - \omega_f^2)(\omega^2 - \omega_s^2)} \right]. \quad (30)$$

It is well known that the linear Hain–Lüst equation possesses singular solutions when $\omega^2 = \omega_a^2$ and $\omega^2 = \omega_h^2$. These are the shear Alfvén and sound continua. Appert *et al.*¹⁴ have shown that the Hain–Lüst equation is regular when $\omega^2 = \omega_f^2$ or $\omega^2 = \omega_s^2$. However, this overlooks the important fact, previously noticed by Grad,¹⁵ that Eqs. (25) and (26) are no longer valid when $\omega^2 = \omega_{f,s}^2$. For the present we shall assume that $\omega^2 \neq \omega_{f,s}^2$ and proceed from Eq. (28).

III. THE NONLINEAR COUPLING EQUATIONS

The nonlinear generalization of the Hain–Lüst equation will now be used to analyze the stability of a finite-amplitude TAE mode. A TAE mode results, for example, from the toroidal coupling of a poloidal harmonic of mode number m with another poloidal harmonic with mode number $m + 1$. Both poloidal modes have the same toroidal mode number n . In cylindrical geometry the m and $m + 1$ poloidal harmonics are independent and both belong to the continuous spectrum of the shear Alfvén wave. Thus, the poloidal modes satisfy the condition

$$\omega^2 = k_{\parallel}^2(r) c_A^2(r), \quad (31)$$

where

$$k_{\parallel}(r) = \frac{1}{R} \left(n - \frac{m}{q(r)} \right). \quad (32)$$

The TAE mode exists in the frequency gap caused by the coupling of the m and $m + 1$ harmonics where the unperturbed frequencies cross, i.e.

$$n - \frac{m}{q(r)} = - \left(n - \frac{m+1}{q(r)} \right). \quad (33)$$

Hence, the TAE mode resulting from the toroidal coupling of the m and $m + 1$ modes is centered on the $q = (m + 1/2)/n$ surface. The two coupled poloidal harmonics have the same parallel wavelength but propagate in opposite directions along the magnetic field. The parallel wave number of the m harmonic is $k_{\parallel}(r) = 1/2q(r)R$ and for the $(m + 1)$ harmonic $k_{\parallel}(r) = -1/2q(r)R$.

The finite-amplitude TAE mode is therefore assumed to vary as

$$A(\mathbf{r}, t) = A_m(r) \exp i \left(\frac{n_a}{R} z - m_a \theta - \omega_a t \right) + A_{m+1}(r) \exp i \left(\frac{n_a}{R} z - (m_a + 1) \theta - \omega_a t \right), \quad (34)$$

where

$$\omega_a^2 \approx k_{\parallel a}^2(r) c_A^2(r), \quad (35)$$

and the radial position where k_{\parallel} and c_A are evaluated is, of course, the $q = (m_a + 1/2)/n_a$ surface. The TAE mode is assumed to exist at finite amplitude due to some unspecified means, although we have in mind the TAE instability due to fusion alpha particles. In discussing the nonlinear stability of such a finite-amplitude TAE mode, attention will be focused on the (m_a, n_a) component. It will be seen that the analysis will be equally applicable to the $(m_a + 1, n_a)$ component.

The mechanism to be analyzed has been discussed previously for the case of a uniform magnetic field in which only one-dimensional variation was considered.¹¹ The present case is much more complicated since the problem is three dimensional and the equilibrium is radially nonuniform. However, it is possible to make analytic progress by taking advantage of the singular nature of the sound waves in ideal MHD. Hence, a density fluctuation is assumed to occur due to noise in the low-frequency spectrum of sound waves. As already mentioned, in ideal MHD sound waves form a continuum whose frequencies are given by $\omega^2 = k_{\parallel}^2(r) c_s^2(r) / (1 + c_s^2/c_A^2)$. The density fluctuation is assumed to occur on the $q = (m_a + 1/2)/n_a$ surface, where the TAE mode is centered. The sound perturbation is localized on the surface and propagates along the magnetic field at the sound speed on the surface. However, the properties of the low-frequency sound wave will be modified due to the presence of the TAE mode. In particular, the TAE mode can beat with the sound wave to produce Alfvén sidebands with frequencies $\omega \pm \omega_a$, where ω is the frequency of the low-frequency density fluctuation. The density perturbation is assumed to have poloidal and toroidal mode numbers (m_h, n_h) so that the sidebands will have $m_h \pm m_a$ and $n_h \pm n_a$ poloidal and toroidal mode numbers. The Alfvén sidebands will be nonresonant, i.e. driven modes, in general. The generated sidebands can also beat with the TAE mode to regenerate the assumed low-frequency density perturbation. Hence, if the sideband fields can be obtained, then a nonlinear equation for the low-frequency sound wave describing its behavior in the presence of a finite-amplitude TAE mode can be derived.

The first task, therefore, is to obtain the equations for the sideband modes. These can be obtained from Eq. (28). By comparing the various nonlinear terms on the right-hand side of this equation, it has been found that there is one term coming from the quantity N that is dominant. This is the term $(B_{0z}/B_0) \rho_1 (\partial^2 \xi_{\theta} / \partial t^2)$ that originates in Eq. (20), the η component of the equation of motion. The dominance of this term arises because the density perturbation ρ_i is one of the main perturbations associated with the sound mode and ξ_{θ} is the most important displacement of the shear Alfvén wave. Clearly, the sidebands must be driven by the beating of a sound wave fluctuation and an Alfvén wave field. In addition, $(B_{0z}/B_0) \sim 1$. The equations for the sidebands can therefore be approximated by

$$\frac{d}{dr} \left(A \frac{d}{dr} (r \xi_r) \right) - C(r \xi_r) \approx \frac{i B_0}{\mu_0} \frac{d}{dr} \left(\frac{G(\omega_g^2 - \omega^2)}{\rho_0 D} \frac{B_{0z}}{B_0} \rho_1^h \frac{\partial^2 \xi_\theta^a}{\partial t^2} \right), \quad (36)$$

where ρ_1^h is the perturbed mass density associated with the sound fluctuation and ξ_θ^a denotes the θ displacement produced by the (n_a, m_a) component of the TAE mode.

The equations for the sidebands ξ_r^\pm can be written as

$$\frac{d}{dr} \left(A_\pm \frac{d}{dr} (r \xi_r^\pm) \right) - C_\pm(r \xi_r^\pm) = \frac{i B_0}{\mu_0} \frac{d}{dr} \left(\frac{G_\pm(\omega_\pm^2 - \omega_{f\pm}^2)}{\rho_0 D_\pm} \frac{B_{0z}}{B_0} \rho_1^h \frac{\partial^2 \xi_\theta^a}{\partial t^2} \right), \quad (37)$$

where

$$A_\pm = \left(\frac{\rho_0(c_s^2 + c_A^2)}{r} \right) \frac{(\omega_\pm^2 - \omega_{a\pm}^2)}{(\omega_\pm^2 - \omega_{f\pm}^2)} \frac{(\omega_\pm^2 - \omega_{h\pm}^2)}{(\omega_\pm^2 - \omega_{s\pm}^2)}, \quad (38)$$

and C_\pm are the corresponding quantities to Eq. (30) with $\omega \rightarrow \omega_\pm$, although we shall not make explicit use of these quantities. Also,

$$G_\pm = - \frac{(m_h \pm m_a)}{r} B_{0z} - \frac{(n_h \pm n_a)}{R} B_{0\theta}, \quad (39)$$

$$D_\pm = (\omega_\pm^2 - \omega_{f\pm}^2)(\omega_\pm^2 - \omega_{s\pm}^2). \quad (40)$$

The frequencies $\omega_{a\pm}$, $\omega_{h\pm}$, $\omega_{f\pm}$, and $\omega_{s\pm}$ are given by

$$\omega_{a\pm}^2 = k_{\parallel\pm}^2 c_A^2, \quad (41)$$

$$\omega_{h\pm}^2 = k_{\parallel\pm}^2 c_s^2 / (1 + c_s^2 / c_A^2), \quad (42)$$

$$\omega_{f,s\pm}^2 = \frac{1}{2} [k_{0\pm}^2 (c_s^2 + c_A^2)] [1 \pm (1 - \alpha_\pm^2)^{1/2}], \quad (43)$$

where

$$\alpha_\pm^2 = \frac{4c_s^2 \omega_{a\pm}^2}{k_{0\pm}^2 (c_s^2 + c_A^2)^2}, \quad (44)$$

$$k_{\parallel\pm} = \frac{1}{R} \left[n_h \pm n_a - \frac{(m_h \pm m_a)}{q(r)} \right], \quad (45)$$

and

$$k_{0\pm}^2 = \frac{(n_h \pm n_a)^2}{R^2} + \frac{(m_h \pm m_a)^2}{r^2}, \quad (46)$$

and $q(r)$ always refers to the $q = (m_a + 1/2)/n_a$ surface and r to the radius of this surface.

The sideband equations can be put into their final form by expressing ρ_1^h in terms of ξ_r^h , and ξ_θ^a in terms of ξ_r^a . Thus, using the linearized continuity equation and the fact that $\xi_{\parallel}^h \gg \eta^h$, the relation between ρ_1^h and ξ_{\parallel}^h is

$$\rho_1^h \approx -i \rho_0 \frac{F_h}{B_0} \xi_{\parallel}^h. \quad (47)$$

Substituting the linear solution for ξ_{\parallel} from Eq. (25) and keeping only the dominant term in $(r \xi_r^h)'$; Eq. (47) becomes

$$\rho_1^h \approx - \frac{\gamma p_0}{B_0^2} \frac{F_h^2}{\omega_{fh}^2} \frac{\omega_{ah}^2}{(\omega_h^2 - \omega_{sh}^2)} \frac{d \xi_r^h}{dr}, \quad (48)$$

where

$$\omega_h^2 = k_{\parallel h}^2 c_s^2 / (1 + c_s^2 / c_A^2), \quad (49)$$

$$F_h^2 = k_{\parallel h}^2 B_0^2, \quad (50)$$

and $\omega_{f,sh}$ correspond to the $\omega_{f,s}$ frequencies for the (m_h, n_h) mode numbers.

The relationship between ξ_θ^a and $(\eta^a, \xi_{\parallel}^a)$ is

$$\xi_\theta^a = \frac{B_{0z}}{B_0} \eta^a + \frac{B_{0\theta}}{B_0} \xi_{\parallel}^a. \quad (51)$$

Since we assume $B_{0z} \gg B_{0\theta}$, we can approximate this to

$$\xi_\theta^a \approx \frac{B_{0z}}{B_0} \eta^a. \quad (52)$$

Again substituting the linear part of Eq. (26) into Eq. (52) and keeping only the derivative term

$$\xi_\theta^a \approx - \frac{i B_{0z} G_a}{B_0^2 (k_{\parallel a}^2 - k_{0a}^2)} \frac{d \xi_r^a}{dr}, \quad (53)$$

where

$$G_a = - \frac{m_a}{r} B_{0z} - \frac{n_a}{R} B_{0\theta}, \quad (54)$$

and $k_{\parallel a}$ and k_{0a} refer to the TAE mode $(-m_a, n_a)$. Substituting Eqs. (48) and (53) into Eq. (37), the required sideband equations are obtained,

$$\frac{d}{dr} \left(A_+ \frac{d}{dr} (r \xi_r^+) \right) - C_+(r \xi_r^+) = \beta_+ \frac{d \xi_r^a}{dr} \frac{d^2 \xi_r^h}{dr^2}, \quad (55)$$

$$\frac{d}{dr} \left(A_- \frac{d}{dr} (r \xi_r^-) \right) - C_-(r \xi_r^-) = \beta_- \left(\frac{d \xi_r^a}{dr} \right)^* \frac{d^2 \xi_r^h}{dr^2}, \quad (56)$$

where * denotes the complex conjugate and

$$\beta_\pm = \mp \frac{G_\pm G_a}{2 \rho_0 \mu_0} \frac{B_{0z}^2 \gamma p_0 k_{\parallel a}^2 k_{\parallel h}^4}{B_0^2 (\omega_h^2 - \omega_{sh}^2) k_{oh}^2 (k_{\parallel a}^2 - k_{0a}^2) (k_{\parallel a}^2 - k_{0\pm}^2)}, \quad (57)$$

where the factor 2 in the denominator of Eqs. (57) comes from the requirement to take the real part explicitly for the product of complex quantities.

To complete the system of coupled nonlinear equations, the corresponding equation for the low-frequency density fluctuation must be obtained. This will also be derived from Eq. (28), but with different nonlinear terms. Again keeping only nonlinear terms with radial derivatives, it is found that the dominant coupling terms come from the θ components of the convective derivative and the $(\mathbf{J}_1 \times \mathbf{B}_1)$ force in the equation of motion and the radial component of the $\mathbf{J}_1 \times \mathbf{B}_1$ force, i.e. the last term on the right-hand side of Eq. (28). In this case the coupling terms must consist of products of sideband quantities and fields associated with the finite-amplitude shear Alfvén wave. The nonlinear low-frequency equation for the sound perturbation is therefore given by

$$\begin{aligned}
& \frac{d}{dr} \left(A_h \frac{d}{dr} (r \xi_r^h) \right) - C_h(r \xi_r^h) \\
& \approx \frac{-iB_0}{2\mu_0} \frac{d}{dr} \left[\frac{G_h(\omega_{gh}^2 - \omega^2)}{\rho_0 D_h} \frac{B_{0z}}{B_0} \right. \\
& \quad \times \left(-\rho_0 \frac{\partial}{\partial t} (\xi_r^a)^* \frac{\partial}{\partial r} \frac{\partial \xi_\theta^+}{\partial t} + \frac{(B_{1r}^a)^*}{\mu_0 r} \frac{\partial}{\partial r} (r B_{1\theta}^+) \right. \\
& \quad \left. \left. - \rho_0 \frac{\partial}{\partial t} \xi_r^a \frac{\partial}{\partial r} \frac{\partial \xi_\theta^-}{\partial t} + \frac{B_{1r}^a}{\mu_0 r} \frac{\partial}{\partial r} (r B_{1\theta}^-) \right) \right] \\
& \quad + \frac{(B_{1\theta}^a)^*}{2\mu_0} \frac{\partial B_{1\theta}^+}{\partial r} + \frac{B_{1\theta}^a}{2\mu_0} \frac{\partial B_{1\theta}^-}{\partial r}, \tag{58}
\end{aligned}$$

where

$$A_h \approx \frac{\rho_0 c_A^2}{r} \frac{\omega_{ah}^2 (\omega^2 - \omega_h^2)}{\omega_{fh}^2 (\omega_h^2 - \omega_{sh}^2)}, \tag{59}$$

$$D_h \approx -\omega_{fh}^2 (\omega_h^2 - \omega_{sh}^2), \tag{60}$$

and ω_{ah}^2 , ω_{gh}^2 , ω_{fh}^2 , and ω_{sh}^2 correspond to the poloidal and toroidal mode numbers of the sound wave perturbation. In order to cast Eq. (58) into its final form, B_{1r}^a is related to ξ_r^a by means of the radial component of the linearized version of Eq. (8), giving

$$B_{1r} \approx i F_a \xi_r^a. \tag{61}$$

Similarly, the following relations hold;

$$\xi_{1\theta}^\pm \approx \frac{B_{0z}}{B_0} \eta^\pm, \tag{62}$$

$$B_{1\theta}^\pm \approx \frac{B_{0z}}{B_0} B_\eta^\pm. \tag{63}$$

Since η^a is the most significant displacement for an Alfvén perturbation, Eq. (15) gives

$$B_\eta^\pm \approx i F_\pm \eta^\pm. \tag{64}$$

Again, retaining only the derivative of the radial displacement in Eq. (26),

$$\eta^\pm \sim -\frac{i G_\pm B_0 \omega_\pm^2}{\rho_0 \mu_0 D_\pm} \frac{d}{dr} \xi_r^\pm. \tag{65}$$

Substituting Eqs. (60)–(65) into Eq. (58) yields the required low-frequency equation,

$$\begin{aligned}
& \frac{d}{dr} \left(A_h \frac{d}{dr} (r \xi_r^h) \right) - C_h(r \xi_r^h) \\
& \approx -\frac{B_0^2}{2\rho_0 \mu_0} \frac{G_h(\omega_{gh}^2 - \omega^2)}{\omega_{fh}^2 (\omega_h^2 - \omega_{sh}^2)} \frac{B_{0z}^2}{\rho_0 \mu_0 B_0^2} \\
& \quad \times \left[\left(\rho_0 \omega_a \omega_+ - \frac{F_a F_+}{\mu_0} \right) \frac{G_+ \omega_+^2}{D_+} \frac{d}{dr} (\xi_r^a)^* \frac{d^2 \xi_r^+}{dr^2} \right. \\
& \quad \left. + \left(\rho_0 \omega_a \omega_- + \frac{F_a F_-}{\mu_0} \right) \frac{G_- \omega_-^2}{D_-} \frac{d}{dr} \xi_r^a \frac{d^2 \xi_r^-}{dr^2} \right] \\
& \quad + \frac{B_0^2}{2\rho_0 \mu_0} \frac{F_a G_a \omega_a^2}{\mu_0 D_a} \frac{B_{0z}^2}{\rho_0 \mu_0 B_0^2} \left[\frac{F_+ G_+ \omega_+^2}{D_+} \left(\frac{d \xi_r^a}{dr} \right)^* \right. \\
& \quad \left. \times \frac{d^2 \xi_r^+}{dr^2} + \frac{F_- G_- \omega_-^2}{D_-} \frac{d \xi_r^a}{dr} \frac{d^2 \xi_r^-}{dr^2} \right], \tag{66}
\end{aligned}$$

where only the radial derivative yielding a second-order equation has been retained.

IV. THE NONLINEAR DISPERSION RELATION

The solution of the coupled equations given by Eqs. (55), (56), and (66) would be very difficult and could only be obtained numerically. In the uniform model¹¹ the corresponding equations were Fourier analyzed, giving algebraic equations. In the present three-dimensional, nonuniform system an approximate nonlinear solution can be obtained by making use of the localization of the sound wave, due to its singular nature, on the $q = (m_a + 1/2)/n_a$ surface, where the finite-amplitude TAE mode is centered. Thus, returning to Eqs. (55) and (56), it is assumed that because ξ_r^h is singular the equations are dominated by the rapid variation of this quantity. With this assumption Eqs. (55) and (56) can be integrated approximately, giving

$$\xi_r^+ \approx \frac{\beta_+}{r A_+} \frac{d \xi_r^a}{dr} \xi_r^h, \tag{67}$$

$$\xi_r^- \approx \frac{\beta_-}{r A_-} \left(\frac{d \xi_r^a}{dr} \right)^* \xi_r^h. \tag{68}$$

The approximate solutions given in Eqs. (67) and (68) may now be substituted into Eq. (66), giving

$$\begin{aligned}
& \frac{d}{dr} \left(A_h \frac{d}{dr} (r \xi_r^h) \right) - C_h(r \xi_r^h) \approx -\frac{B_0^2}{2\rho_0 \mu_0} \frac{B_{0z}^2}{\rho_0 \mu_0 B_0^2} \left[\left[\frac{G_h(\omega_{gh}^2 - \omega^2)}{\omega_{fh}^2 (\omega_h^2 - \omega_{sh}^2)} \left(\rho_0 \omega_a \omega_+ - \frac{F_a F_+}{\mu_0} \right) - \frac{F_a G_a \omega_a^2 F_+}{\mu_0 D_a} \right] \frac{G_+ \omega_+^2}{D_+} \frac{\beta_+}{r A_+} \right. \\
& \quad \left. + \left[\frac{G_h(\omega_{gh}^2 - \omega^2)}{\omega_{fh}^2 (\omega_h^2 - \omega_{sh}^2)} \left(\rho_0 \omega_a \omega_- + \frac{F_a F_-}{\mu_0} \right) - \frac{F_a G_a \omega_a^2 F_-}{\mu_0 D_a} \right] \frac{G_- \omega_-^2}{D_-} \frac{\beta_-}{r A_-} \right] \left| \frac{d \xi_r^a}{dr} \right|^2 \frac{d^2 \xi_r^h}{dr^2}. \tag{69}
\end{aligned}$$

The nonlinear dispersion relation is now obtained from the consistency condition that the low-frequency sound wave is a singular mode in the presence of the finite-amplitude TAE mode. This requires the coefficient of $(d^2 \xi_r^h / dr^2)$ in Eq. (69) to equal zero on the original magnetic surface, $q_a = (m_a + 1/2)/n_a$. Hence, the dispersion relation is

$$rA_h + \frac{B_0^2}{4\rho_0\mu_0} \frac{B_{0z}^2}{\rho_0\mu_0 B_0^2} \left\{ \left[\frac{G_h(\omega_{gh}^2 - \omega_h^2)}{\omega_{fh}^2(\omega_h^2 - \omega_{sh}^2)} \left(\rho_0\omega_a\omega_+ - \frac{F_a F_+}{\mu_0} \right) - \frac{F_a G_a \omega_a^2 F_+}{\mu_0 D_a} \right] \frac{G_+ \omega_+^2}{D_+} \frac{\alpha_+}{rA_+} \right. \\ \left. + \left[\frac{G_h(\omega_{gh}^2 - \omega_h^2)}{\omega_{fh}^2(\omega_h^2 - \omega_{sh}^2)} \left(\rho_0\omega_a\omega_- + \frac{F_a F_-}{\mu_0} \right) - \frac{F_a G_a \omega_a^2 F_-}{\mu_0 D_a} \right] \frac{G_- \omega_-^2}{D_-} \frac{\alpha_-}{rA_-} \right\} \left| \frac{d\xi_r^a}{dr} \right|^2 = 0, \quad (70)$$

which is a local dispersion relation referring to the $q = (m_a + 1/2)/n_a$ surface. Substituting for A_\pm , D_\pm , β_\pm and A_h from Eqs. (38), (40), (57), and (59), respectively, into Eq. (70), the equation becomes

$$\rho_0 \frac{\omega_{ah}^2}{\omega_{fh}^2} \frac{(\omega^2 - \omega_h^2)}{(\omega_h^2 - \omega_{sh}^2)} + \frac{B_0^2}{4\rho_0\mu_0} \frac{B_{0z}^2}{\rho_0\mu_0 B_0^2} \frac{G_a}{\rho_0\mu_0} \frac{B_{0z}^2}{B_0^2} \gamma p_0 \\ \times \frac{k_{\parallel a}^2 k_{\parallel h}^4}{k_{0h}^2 (k_{\parallel a}^2 - k_{0a}^2) (\omega_h^2 - \omega_{sh}^2)} \left[- \left(\frac{G_h(\omega_{gh}^2 - \omega_h^2)}{\omega_{fh}^2(\omega_h^2 - \omega_{sh}^2)} \rho_0(\omega_a^2 - k_{\parallel a} k_{\parallel} + c_A^2) - \rho_0 k_{\parallel a} k_{\parallel} + c_A^2 \omega_a^2 \frac{G_a}{D_a} \right) \right. \\ \times \frac{G_+ \omega_a^2}{\rho_0 c_A^2 (\omega_a^2 - \omega_{a+}^2) (k_{\parallel a}^2 - k_{0+}^2) \omega_a^2} + \left(\frac{G_h(\omega_{gh}^2 - \omega_h^2)}{\omega_{fh}^2(\omega_h^2 - \omega_{sh}^2)} \rho_0(\omega_a^2 + k_{\parallel a} k_{\parallel} - c_A^2) - \rho_0 k_{\parallel a} k_{\parallel} - c_A^2 \omega_a^2 \frac{G_a}{D_a} \right) \\ \left. \times \frac{G_- \omega_a^2}{\rho_0 c_A^2 (\omega_a^2 - \omega_{a-}^2) \omega_a^2 (k_{\parallel a}^2 - k_{0-}^2)} \right] \left| \frac{d\xi_r^a}{dr} \right|^2 = 0, \quad (71)$$

where $\omega_\pm = \omega_a \pm \omega \approx \omega_a$. In order to put Eq. (71) into its final form, we use the result

$$\frac{(\omega_{gh}^2 - \omega_h^2)}{(\omega_h^2 - \omega_{sh}^2)} = - \frac{k_{0h}^2}{k_{\parallel h}^2}, \quad (72)$$

and introducing the wave number k_η through the relation

$$G = k_\eta B_0, \quad (73)$$

we can write

$$G_h = k_{\eta h} B_0, \quad (74)$$

$$G_a = k_{\eta a} B_0, \quad (75)$$

$$G_\pm = k_{\eta\pm} B_0. \quad (76)$$

The final form of the nonlinear dispersion relation is now obtained by substituting Eqs. (35) and (41) for ω_a^2 and $\omega_{a\pm}^2$ and Eqs. (72)–(76) into Eq. (71), giving

$$\omega^2 \approx \omega_h^2 - \frac{k_{\eta a} k_{\eta h} c_s^2 k_{\parallel a}^2}{4(k_{0a}^2 - k_{\parallel a}^2)} \left(\frac{k_{\parallel a} k_{\eta+}^2}{(k_{\parallel a} + k_{\parallel+}) (k_{0+}^2 - k_{\parallel a}^2)} \right. \\ \left. - \frac{k_{\parallel a} k_{\eta-}^2}{(k_{\parallel a} - k_{\parallel-}) (k_{0-}^2 - k_{\parallel a}^2)} \right) \left| \frac{d\xi_r^a}{dr} \right|^2 \\ - \frac{k_{\eta a}^2 c_s^2 k_{\parallel a}^2 k_{\parallel h}^2}{4(k_{0a}^2 - k_{\parallel a}^2)^2} \left(\frac{k_{\parallel a} k_{\parallel} + k_{\eta+}^2}{(k_{\parallel+}^2 - k_{\parallel a}^2) (k_{0+}^2 - k_{\parallel a}^2)} \right. \\ \left. - \frac{k_{\parallel a} k_{\parallel} - k_{\eta-}^2}{(k_{\parallel a}^2 - k_{\parallel-}^2) (k_{0-}^2 - k_{\parallel a}^2)} \right) \left| \frac{d\xi_r^a}{dr} \right|^2. \quad (77)$$

The dispersion relation given in Eq. (77) has a structure similar to the corresponding uniform case.¹¹ This was partly expected because of the treatment of a singular mode on a particular flux surface. For the choice made of positive toroidal mode numbers and negative poloidal mode numbers, the values of k_{\parallel} will usually be positive and those of k_η negative. It is clear that $k_{0a}^2 - k_{\parallel a}^2 > 0$ and $k_{0+}^2 - k_{\parallel a}^2 > 0$. It is

also the case that $k_{0-}^2 - k_{\parallel a}^2 > 0$, except for a particular choice of mode numbers such as $m_h = m_a$. Thus, both terms in Eq. (77) related to the finite-amplitude TAE mode will be negative when $k_{\parallel-} > k_{\parallel a}$, where

$$k_{\parallel-} = \frac{1}{R} \left(n_h - n_a - \frac{(m_h - m_a)}{q(r)} \right). \quad (78)$$

The singular density perturbation will therefore be unstable for $k_{\parallel-} > k_{\parallel a}$ when $|d\xi_r^a/dr|$ is above the threshold implied by Eq. (77). Above this threshold, not only the density fluctuation grows in time but also the driven sideband modes. The general expression for the threshold amplitude will be rather complicated. As an example, we therefore evaluate the threshold for a specific case where $k_{\parallel h} = 3k_{\parallel a}$ corresponding to toroidal and poloidal mode numbers for the density perturbation $n_h = 3n_a$, $m_h = 3m_a$. For these conditions $k_{\eta a} \approx m_a/r$, $k_{\eta h} \approx 3m_a/r$ and $k_{\eta+} \approx 4m_a/r$, $k_{\eta-} \approx 2m_a/r$, where use has been made of the tokamak ordering $B_{0z} \gg B_{0\theta}$ and $r/R \ll 1$. With these assumptions we find $k_{0a}^2 - k_{\parallel a}^2 \approx m_a^2/r^2$, $k_{0-}^2 - k_{\parallel a}^2 \approx 4m_a^2/r^2$ and $k_{0+}^2 - k_{\parallel a}^2 \approx 16m_a^2/r^2$. The threshold amplitude can be obtained from Eq. (77) when $\omega^2 = 0$. In order to obtain the threshold in terms of B_{1r}^a/B_0 , where B_{1r}^a is the radial component of the perturbed magnetic field produced by the TAE mode, we approximate

$$\frac{d\xi_r^a}{dr} \approx \frac{m_a}{r} \xi_r^a,$$

and using Eq. (17),

$$|\xi_r^a| = \frac{1}{k_{\parallel a}} \frac{B_{1r}^a}{B_0}. \quad (79)$$

The threshold amplitude for the modulational instability is therefore given by the approximate expression

$$\left| \frac{B_{1r}^a}{B_0} \right|^2 \approx \frac{5}{2} \frac{1}{q^2} \frac{r^2}{R^2} \frac{1}{m_a^2}, \quad (80)$$

where a term proportional to $k_{\parallel a}^2 r^2 / m_a^2$ has been neglected and q is the safety factor of the flux surface under consideration. For $m_a = 20$, $r/R = 0.1$ (as in Ref. 9) and $q = 2$,

$$\left| \frac{B_{1r}^a}{B_0} \right| \simeq 4 \times 10^{-3}. \quad (81)$$

This is to be compared with a value of 10^{-3} obtained in Ref. 9. However, as we shall indicate in a moment, the threshold value given in Eq. (81) can be significantly lower than this typical value. Hence, the modulational instability of a TAE wave is a possible mechanism for the saturation of the initial instability. The result of the modulational instability would be to produce a purely growing (zero-frequency) density perturbation on the flux surface on which the TAE mode is centered. The sideband magnetic fluctuations that would also grow, due to the modulational instability, would cause a spatially periodic modulation of the magnetic field fluctuations of the initial TAE mode. These fluctuations would be strong in regions of low density and weak in regions of increased density.

The threshold amplitude given in Eq. (81) has been obtained for a particular choice of $k_{\parallel h} = 3k_{\parallel a}$. However, the dispersion relation given in Eq. (77) shows that the threshold could be significantly lower. In particular, for $k_{\parallel -} = k_{\parallel a}$ (or $k_{\parallel h} = 2k_{\parallel a}$) the threshold becomes formally zero. At this point the theory, as presented, breaks down since it has been assumed that $\omega \ll \omega_a$. Nevertheless, it is clear that this case corresponds to a resonant decay instability, first discussed in Ref. 10, in which an Alfvén wave and a low-frequency sound wave are excited by the initial TAE wave. The lower sideband has become resonant and the frequency and wave number matching conditions $\omega_0 = \omega_1 + \omega_s$, $\mathbf{k}_0 = \mathbf{k}_1 + \mathbf{k}_s$ are satisfied, where (ω_0, \mathbf{k}_0) is the TAE (large-amplitude) wave and (ω_1, \mathbf{k}_1) , (ω_s, \mathbf{k}_s) are the lower Alfvén sideband and the resonant sound wave, respectively.

The resonant case can be dealt with by introducing dissipation into Eq. (77). The simplest procedure for doing this is to follow Ref. 11 and include a phenomenological collision term in the low-frequency sound wave response and resistivity in the resonant Alfvén term. Thus, $\omega^2 - \omega_h^2 \rightarrow \omega^2 - \omega_h^2 + i\omega\nu$ and $k_{\parallel a} - k_{\parallel -} \rightarrow k_{\parallel a} - k_{\parallel -} + ik_{\parallel -}^2 \eta \omega_- / [\mu_0 c_A^2 (k_{\parallel a} + k_{\parallel -})]$, where ν is a phenomenological collision frequency that could simulate ion Landau damping, and η is the resistivity. The introduction of a phenomenological damping term for the sound waves is in the spirit of a ‘‘proof of principle’’ fluid calculation. Of course, collisionless kinetic effects are likely to be important for the damping of sound waves. However, the presence of inhomogeneity or an equilibrium flow can reduce the strength of the kinetic damping or even reverse its sign if the sound frequency is less than the diamagnetic drift frequency of the bulk ions. In any case, the present calculation is heuristic, where the principal aim is to identify the conditions when mode coupling saturation is important.

With the above replacements the threshold at resonance can be obtained making the same approximations as for the nonresonant case. The result is

$$\left| \frac{B_{1r}^a}{B_0} \right|^2 = \frac{2\eta\nu}{\mu_0 c_S c_A} \left(\frac{k_{\parallel a} r}{m_a} \right)^2. \quad (82)$$

This is larger than the uniform field result by the factor c_A/c_S but smaller by the factor $(k_{\parallel r}/m_a)^2$.

The threshold condition given in Eq. (82) can also be written in terms of the damping rates of the Alfvén and sound waves. The Alfvén damping rate is given by

$$2\gamma_A \simeq \frac{\eta k_{\parallel a}^2}{\mu_0}, \quad (83)$$

and the damping rate γ_s of the sound wave by

$$2\gamma_s \simeq \nu. \quad (84)$$

Substituting Eqs. (83) and (84) into Eq. (82), we obtain

$$\left| \frac{B_{1r}^a}{B_0} \right|^2 = \frac{8\gamma_s}{\omega_s} \frac{\gamma_A}{\omega_A} \frac{k_{\parallel h} k_{\parallel a} r^2}{m_a^2}, \quad (85)$$

where γ_s and γ_A can be interpreted, for example, as due to ion Landau damping. For sound waves in an isothermal plasma, $\gamma_s/\omega_s \sim 1$, but $\gamma_A/\omega_A \ll 1$ and $k_{\parallel h} k_{\parallel a} r^2 / m_a^2 \ll 1$, giving rise to even lower thresholds than the typical value given by Eq. (81).

To conclude this section let us consider the matching conditions that must be satisfied for the resonance to occur. We have seen that the resonance is given approximately by $k_{\parallel -} = k_{\parallel a}$, which corresponds to toroidal and poloidal mode numbers for the density perturbation $n_h = 2n_a$, $m_h = 2m_a$. We therefore assume

$$n_h = 2n_a + \delta n, \quad (86)$$

$$m_h = 2m_a + \delta m. \quad (87)$$

Substituting Eqs. (86) and (87) into Eq. (78), we obtain

$$k_{\parallel -} = \frac{1}{2qR} + \frac{1}{R} \left(\delta n - \frac{\delta m}{q} \right). \quad (88)$$

With the aid of the frequency and wave number matching conditions, we obtain

$$\delta n - \frac{\delta m}{q} = -\frac{1}{q} \frac{c_S}{c_A}. \quad (89)$$

For a low- β plasma this condition cannot be satisfied if $\delta n = 0$. However, for $\delta n = 1$,

$$\delta m = q + \frac{c_S}{c_A}. \quad (90)$$

Making use of the result, $q = (2m_a + 1)/2n_a$, we find that Eq. (90) can be satisfied for $c_S/c_A = 0.1$, $m_a = 9$, $n_a = 5$ if $\delta m = 2$. Similarly, for $\delta n = -1$,

$$\delta m = -q + \frac{c_S}{c_A}, \quad (91)$$

and this condition can again be satisfied for $c_S/c_A = 0.1$, $m_a = 10$, $n_a = 5$ if $\delta m = -2$.

V. SUMMARY AND CONCLUSIONS

In this paper we have considered a mode coupling mechanism for the saturation of a TAE instability. This mechanism provides a channel for the finite-amplitude TAE wave, which obtains its energy from the fusion alpha particles, to transfer this energy to other modes of the plasma. This will occur once the TAE wave has reached the threshold amplitude for modulational instability. As a result, the amplitude of the TAE wave will saturate close to the modulational threshold level so that additional energy flowing into the TAE wave from the alpha particles will be transferred to these other fluctuations.

The mechanism of the modulational instability of a finite-amplitude TAE wave is as follows. A low-frequency density fluctuation with frequency ω and wave vector \mathbf{k}_h is assumed to occur at noise level. The density fluctuation beats with the TAE wave (ω_a, \mathbf{k}_a) to produce sidebands ($\omega_a \pm \omega, \mathbf{k}_a \pm \mathbf{k}_h$). In their turn, the sideband fluctuations beat with the finite-amplitude TAE wave to regenerate the original density fluctuation, thus closing the feedback loop. The nonlinear coupled equations for this process yield a nonlinear dispersion relation, given by Eq. (77), which contains a term proportional to the intensity of the TAE wave. If this amplitude is allowed to become zero, the dispersion relation reduces to the equation for linear sound waves. However, Eq. (77) shows that for $k_{\parallel h} > 2k_{\parallel a}$, the frequency of the density fluctuation is downshifted to zero and the fluctuations become unstable provided the amplitude of the TAE wave exceeds the threshold given by Eq. (81) for the case $k_{\parallel h} = 3k_{\parallel a}$. As $k_{\parallel h} \rightarrow 2k_{\parallel a}$ from above, the threshold becomes progressively lower and formally reaches zero when $k_{\parallel h} = 2k_{\parallel a}$, corresponding to the lower sideband becoming resonant with an Alfvén wave propagating in the opposite direction to the TAE wave. This is in fact the decay instability for which the sound wave is excited at its natural frequency.¹⁰ The resonant case has been treated by introducing resistivity and a phenomenological collision frequency into the ideal MHD model. This allowed a finite threshold to be calculated in terms of the damping rates of the Alfvén and sound waves. Although the resonant case requires the frequency and wave number matching relations to be satisfied for the bounded system we showed that these conditions can be met for parameters relevant to present large tokamaks. A more precise calculation would need to include the details of the frequency shift of the TAE mode due to the toroidal coupling which has been neglected in the present cylindrical calculation.

The nonlinear dispersion relation given by Eq. (77) was obtained by making a number of simplifying approximations. The most important of these made use of the fact that in ideal MHD, sound waves form a continuum of singular modes. Each mode is centered on a particular flux surface and propagates along the magnetic field at the sound speed corresponding to that particular surface. The sound fluctuation has therefore been assumed to occur on the same magnetic surface as that on which the TAE mode is centered. The nonlinear dispersion relation has been obtained by assuming that the density fluctuation remains a singular mode in the presence of the TAE wave. The calculation is therefore carried out on one magnetic flux surface, thus enabling an analytic result to be obtained. The low threshold amplitude implied by this calculation suggests that the modulational instability may be a significant saturation mechanism for TAE instabilities.

In conclusion, one further observation is made, concerning the spectrum of modes of ideal MHD. The single fluid MHD system is known to be self-adjoint in the absence of equilibrium flows. In this case ω^2 must be real. All unstable modes (with $\omega^2 < 0$) always belong to the discrete spectrum since the governing differential equations have no singularities within the solution domain. When $\omega^2 > 0$, the Hain–Lüst equation for ξ_r has singularities only at $\omega^2 = \omega_a^2$ and $\omega^2 = \omega_h^2$ and not at $\omega^2 = \omega_{f,s}^2$ (Appert *et al.*¹⁴). In view of this, it can be concluded that two continua arise from these singularities. However, the continuous spectrum associated with ideal MHD arises from all the singular points of the system and not merely those at the Hain–Lüst singularities. We thus find that at $\omega^2 = \omega_{f,s}^2$ a new class of Case–Van Kampen¹⁶ continua is obtained, as suggested by Grad.¹⁵ The new Case–Van Kampen continua arise in Eqs. (25) and (26) when $D = 0$, i.e. when $\omega^2 = \omega_{f,s}^2$. These can, in principle, have important new consequences, not only for the modulational instability problem discussed in the present paper, but also, more generally, for continuum damping of TAEs, Alfvén wave heating, etc. The theory of these new continua and their consequences will be considered in later work.

ACKNOWLEDGMENTS

This work was partly supported by the UK Department of Trade and Industry and Euratom, and the Engineering and Physical Sciences Research Council Grant No. GR/K58937.

APPENDIX

The quantities N and L appearing in Eqs. (23) and (24) are given by

$$\begin{aligned}
 N = & \frac{iF}{\mu_0} \left\{ -\frac{iB_{0z}}{\omega B_0} \frac{\partial}{\partial r} \left(B_{1\theta} \frac{\partial \xi_r}{\partial t} - B_{1r} \frac{\partial \xi_\theta}{\partial t} \right) - \frac{iB_{0\theta}}{\omega B_0} \frac{1}{r} \frac{\partial}{\partial r} \left[r \left(B_{1r} \frac{\partial \xi_z}{\partial t} - B_{1z} \frac{\partial \xi_r}{\partial t} \right) \right] \right\} - \frac{iG}{\mu_0} \left\{ -\frac{iB_{0\theta}}{\omega B_0} \frac{\partial}{\partial r} \left(B_{1\theta} \frac{\partial \xi_r}{\partial t} - B_{1r} \frac{\partial \xi_\theta}{\partial t} \right) \right. \\
 & + \frac{iB_{0z}}{\omega B_0} \frac{1}{r} \frac{\partial}{\partial r} \left[r \left(B_{1r} \frac{\partial \xi_z}{\partial t} - B_{1z} \frac{\partial \xi_r}{\partial t} \right) \right] - \frac{B_{0z}}{B_0} \rho_1 \frac{\partial^2 \xi_\theta}{\partial t^2} - \frac{B_{0z}}{B_0} \rho_0 \frac{\partial \xi_r}{\partial t} \frac{\partial^2 \xi_\theta}{\partial r \partial t} + \frac{B_{0z}}{B_0} \frac{B_{1r}}{\mu_0 r} \frac{\partial}{\partial r} (r B_{1\theta}) + \frac{B_{0\theta}}{B_0} \rho_1 \frac{\partial^2 \xi_z}{\partial t^2} \\
 & \left. + \frac{B_{0\theta}}{B_0} \rho_0 \frac{\partial \xi_r}{\partial t} \frac{\partial^2 \xi_z}{\partial r \partial t} - \frac{B_{0\theta}}{B_0} \frac{B_{1r}}{\mu_0} \frac{\partial B_{1z}}{\partial r} \right\}, \tag{A1}
 \end{aligned}$$

$$L = -\frac{B_{0\theta}}{B_0} \rho_1 \frac{\partial^2 \xi_\theta}{\partial t^2} - \frac{B_{0\theta}}{B_0} \rho_0 \frac{\partial \xi_r}{\partial t} \frac{\partial^2 \xi_\theta}{\partial r \partial t} + \frac{B_{0\theta} B_{1r}}{B_0 \mu_0 r} \frac{\partial}{\partial r} (r B_{1\theta}) - \frac{B_{0z}}{B_0} \rho_1 \frac{\partial^2 \xi_z}{\partial t^2} - \frac{B_{0z}}{B_0} \rho_0 \frac{\partial \xi_r}{\partial t} \frac{\partial^2 \xi_z}{\partial r \partial t} + \frac{B_{0z} B_{1r}}{B_0 \mu_0} \frac{\partial B_{1z}}{\partial r}. \quad (\text{A2})$$

¹C. Z. Cheng, L. Chen, and M. S. Chance, *Ann. Phys. (N.Y.)* **161**, 21 (1984).

²G. Y. Fu and J. W. Van Dam, *Phys. Fluids* **30**, 1949 (1989).

³R. Nazikian, G. Y. Fu, S. H. Batha, M. G. Bell, R. E. Bell, R. V. Budny, C. E. Bush, Z. Chang, Y. Chen, C. Z. Cheng, D. S. Darrow, P. C. Efthimion, E. D. Fredrickson, N. N. Gorelenkov, B. Leblanc, F. M. Levinton, R. Majeski, E. Mazzucato, S. S. Medley, H. K. Park, M. P. Petrov, D. A. Spong, J. D. Strachan, E. J. Synakowski, G. Taylor, S. Von Goeler, R. B. White, K. L. Wong, and S. J. Zweben, *Phys. Rev. Lett.* **78**, 2976 (1997).

⁴D. J. Grove and D. M. Meade, *Nucl. Fusion* **32**, 187 (1992).

⁵Technical Basis for the ITER Interim Design Report, Cost Review and Safety Analysis (International Atomic Energy Agency, Vienna, 1996).

⁶H. L. Berk and B. N. Breizman, *Phys. Fluids B* **2**, 2246 (1990).

⁷G. Vlad, C. Kar, F. Zonca, and F. Romanelli, *Phys. Plasmas* **2**, 418 (1995).

⁸D. A. Spong, B. A. Carreras, and C. L. Hedrick, *Phys. Plasmas* **1**, 1503 (1994).

⁹T. S. Hahm and L. Chen, *Phys. Rev. Lett.* **74**, 266 (1995).

¹⁰A. A. Galeev and V. N. Oraevskii, *Dokl. Akad. Nauk SSSR* **147**, 71 (1962); *Sov. Phys. Dokl.* **7**, 988 (1963).

¹¹C. N. Lashmore-Davies, *Phys. Fluids* **19**, 587 (1976).

¹²K. Hain and R. Lüst, *Z. Naturforsch. A* **13a**, 936 (1958).

¹³J. P. Freidberg, *Ideal Magnetohydrodynamics* (Plenum Press, New York, 1987), p. 473.

¹⁴K. Appert, R. Gruber, and J. Vaclavik, *Phys. Fluids* **17**, 1471 (1974).

¹⁵H. Grad, *Proc. Natl. Acad. Sci. USA* **70**, 3277 (1973).

¹⁶N. G. Van Kampen and B. U. Felderhof, *Theoretical Methods in Plasma Physics* (North-Holland, Amsterdam, 1967), p. 139.